A Strategy for Reduction of Streak Artifacts in Low-dose CT

Tianfang Li, Xiang Li, Yuxiang Xing, Hongbing Lu, Jiang Hsieh, and Zhengrong Liang

***Abstract*--** Streak artifacts have been one of the major classes of image artifacts resulting from excessive quantum noise in low-dose x-ray CT. It has been shown that, to treat the noise in low-dose CT more accurately, both the analysis of the noise properties of the projection data and the development of a corresponding efficient filtering method are necessary. From our previous analysis of the calibrated low-dose CT projection data, it was clearly seen that the data could be regarded as approximately Gaussian distributed with nonlinear signal-dependent variance. Based on this observation, a penalized weighted least square (WLS) statistic framework was chosen for an optimal solution. In this work, we further incorporated a novel *a priori* idea into the framework, which can accurately preserve more information in high-noise regions with a significant reduction of the streak artifacts. This new penalty term was directly calculated from the sinogram. The method was tested by experimental data acquired at 120 kVp and 10 mA protocols, demonstrating a significant reduction on streak artifacts and noise suppression without sacrificing the spatial resolution.

I. Introduction

STREAK artifacts have been one of the major classes of image artifacts resulting from excessive x-ray quantum noise in low-dose x-ray CT (Computed Tomography). The reason is that, when several large and dense objects are present in the scanning field of view (FOV), for certain paths, it is more difficult for the x-ray photons to pass through and reach the detector. For example, if a patient's arms are inside the FOV, and when the x-ray tube is at 3 o'clock or 9 o'clock position, x-ray photons have to pass both shoulder/arm bones and an extremely long soft tissue path before exiting the patient. As a result, very few x-ray photons can reach the detector [1]. Therefore, there are often some extremely noisy regions in the sinogram, which lead to streak artifacts in the reconstructed image.

Figure 1(a) showed one slice of a shoulder phantom "raw" data collected with GE high-speed multi-slice spiral CT operated at 120kVp and 10mA. The data was after machine calibration and logarithm-transformation. We can easily identify the two extremely noisy regions (denoted by A) from the picture, which lead to streak artifacts in the reconstructed image showed in Figure 3(a). It is worthy to point out that the other region of the sinogram is quite smooth compared with region A. To emphasize this, the projections from view angle 0^0 and from view angle 90^0 were plot in Figure 1 (b) and (c), where the different SNR (signal to noise ratio) was observed.

Considering the low-count nature of this modality with signal-dependent noise contamination, conventional approaches for the noise reduction by spatially invariant, low-pass filters to smooth each projection image separately generate sub-optimal solutions in this situation. Up to now, various forms of filtering techniques have been developed to spatially smooth the projection data and/or the reconstructed CT images, such as the adaptive trimmed mean filter, the non-linear anisotropic diffusion filter, etc. [1,2] Although they succeed in some degrees for noise reduction prior or post to image reconstruction, the assumption of the noise model is not justified in their applications and further development is then limited. It has been shown that, to treat the noise in low-dose CT more accurately, the analysis of the noise properties of the projection data and the development of a corresponding efficient filtering method are two major problems to be addressed.

From our previous works on analyzing the noise properties of calibrated low-dose CT projection data, it is clearly seen that the data can be regarded as approximately Gaussian distributed with a nonlinear signal-dependent variance [3]. Based on this observation, a penalized weighted least-square (WLS) statistic framework is the choice for an optimal solution. In this work, we further incorporate a novel *a priori* which can accurately preserve more information in the high-noise regions characterized by the streak artifacts. This new prior information is directly calculated from the sinogram. Experimental study with GE multi-slice spiral CT data collected at 10 mA showed satisfactory result using our proposed method.

Manuscript submitted on October 20, 2003. This work was supported in part by the NIH National Heart, Lung and Blood Institute under Grant No. HL54166 and the NIH National Cancer Institute under Grant No. CA82402.

T. Li is with the Departments of Physics and Astronomy and Radiology, State University of New York, Stony Brook, NY 11790 USA (telephone: 631-444-7999, e-mail: tfli@mil.sunysb.edu).

X. Li was with the Department of Radiology, State University of New York at Stony Brook, and now is with the Department of Radiation Therapy, Columbia University, USA.

Z. Liang is with the Departments of Radiology and Computer Science, State University of New York, Stony Brook, NY 11794, USA.

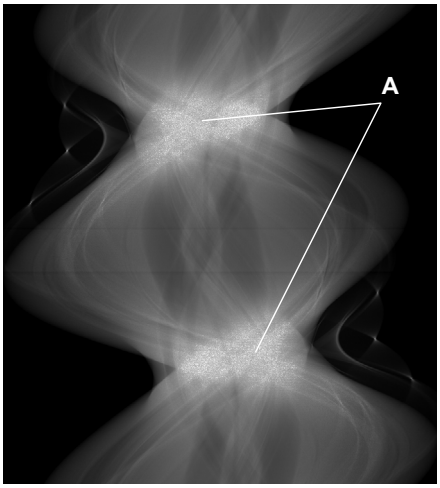

(a)

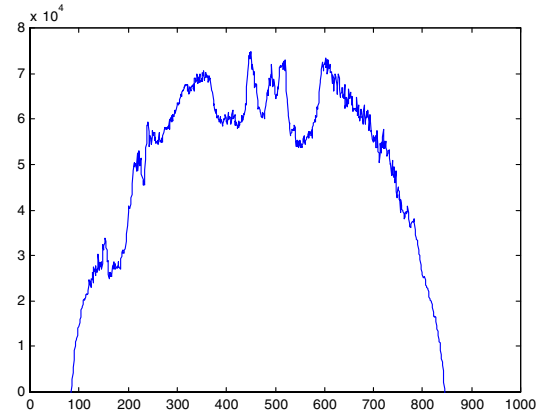

(b)

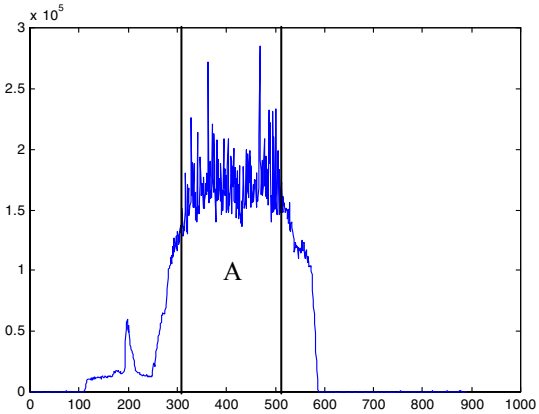

(c)

Fig. 1. Sinogram of a shoulder phantom as scanned by a GE multi-slice spiral CT system at 120kVp and 10mA protocol. Picture (a) is 360^0 scan data, and A identifies the noisier region. Profiles (b) and (c) were drawn from the sinogram (a), where (b) is for view angle 0^0 and (c) is for view angle 90^0, respectively. We can observe that the projection at angle 0^0 is much more smooth as compared with projection at angle 90^0. The extremely noisy region A in profile (c) is because that rays in this region passed through bones and longer soft tissues.

II. THEORY

In this section, we first briefly discussed the statistical frameworks of maximum likelihood (ML) and maximum a posteriori (MAP) for sinogram image restoration. Then a new *a priori* idea was presented for preserving more useful information in the process. The new *a priori* reflected the unique property of a sinogram image.

A. Maximum Likelihood Estimation

For an x-ray CT sinogram, the data scanned at each view and each channel (detector element) can be considered as a statistic independent random process x_i, which was proved to follow Gaussian distribution with mean μ_i and variance σ_i^2 [3]:

$$p(x_i) = \frac{1}{\sqrt{2\pi\sigma_i}} \exp(-\frac{(x_i-\mu_i)^2}{2\sigma_i^2}) \qquad (1)$$

therefore, the log-likelihood is

$$LL = -\sum_i \left(\frac{(x_i-\mu_i)^2}{2\sigma_i^2} + \frac{1}{2}\ln(\sigma_i^2) + \frac{1}{2}\ln(2\pi) \right). \qquad (2)$$

It is easy to see that the maximum likelihood (ML) solution for μ_i is x_i itself, if the mean μ_i and the variance σ_i^2 were irrelative. However, from the literatures [3,4,5] and our previous analysis [2], it can be found that the variance is exponentially proportional to the mean

$$\sigma_i^2 = b\exp(a\mu_i) \qquad (3)$$

where *a* and *b* are system dependent (but object independent) constants. Taking derivative with respect to the mean μ_i yield the following equation

$$(\hat{\mu}_i - (x_i + \frac{1}{a}))^2 - \frac{1}{a^2} = b\exp(a\hat{\mu}_i). \qquad (4)$$

where the solution $\hat{\mu}_i$ can be easily obtained by using Newton-Raphson method.

Sinogram restored by ML estimation can be regarded as the result of shifting the observed data x_i by a certain amount which is only determined by its own variance value. Hence, there is usually no any denoising effect in the resulted image.

B. Maximum A Posteriori (MAP) Estimation

One commonly used Bayesian approach in image denoising is the maximum *a posteriori* (MAP) estimation method which incorporates prior information. Denote by $P(\mu)$ the prior distribution for the unknown image $\mu = \{\mu_1, \mu_2, \cdots, \mu_N\}^T$ (*N* is total number of pixels in the sinogram). Let *X* be the observed sinogram image $X = \{x_1, x_2, \cdots x_N\}^T$, the MAP estimator is given by

$$\hat{\mu} = \arg\max_{\mu\geq 0}\{P(\mu|X)\} = \arg\max_{\mu\geq 0}\{P(X|\mu)P(\mu)\} \qquad (5)$$

where the Bayesian formula is used

$$P(\mu|X) = \frac{P(X|\mu)P(\mu)}{P(X)} \propto P(X|\mu)P(\mu). \qquad (6)$$

It can be assumed that the observation at each pixel was independent of the other observations [4], so that the conditional probability of observed image *X* given mean image μ can be simply expressed as

$$P(X|\mu) = \prod_{i=1}^{N} p(x_i|\mu_i) \qquad (7)$$

A general model for the prior distribution $P(\mu)$ is a *Markov random field* (MRF) which is characterized by its Gibbs distribution given by [5]

$$P(\mu) = \frac{1}{Z}\exp(-\frac{\alpha}{2}\mu^T H\mu) \qquad (8)$$

usually implemented in the MAP estimation method. This method regularizes its solution to be smooth in any region.

Here, *Z* is a constant and α is weighting parameter. *H* is *N*N* square matrix, which has low-pass property. For the 2D image, the core function of matrix *H* is often designed as [6]

$$\begin{bmatrix} -\frac{\sqrt{2}}{2} & -1 & -\frac{\sqrt{2}}{2} \\ -1 & 4+2\sqrt{2} & -1 \\ -\frac{\sqrt{2}}{2} & -1 & -\frac{\sqrt{2}}{2} \end{bmatrix} \qquad (9)$$

By taking logarithm transformation, the MAP estimation became a penalized WLS problem [7]:

$$\Phi(\mu) = \frac{1}{2}(X-\mu)^T\Sigma^{-1}(X-\mu) + \frac{1}{2}\mu^T H\mu$$
$$\hat{\mu} = \arg\min_{\mu\geq 0}\Phi(\mu) \qquad (10)$$

where $\Phi(\mu)$ denotes the cost function. The variance-covariance matrix Σ is diagonal with the *i*th entry σ_i^2.

Again, if the variance σ_i^2 is irrelative to the mean μ_i, there is a simple closed-form solution

$$\hat{\mu} = (\Sigma^{-1} + \alpha H)^{-1}\Sigma^{-1}X \qquad (11)$$

If considering the variance dependence on the mean value, the MAP estimation will result in nonlinear sets of equations, which will be complicated to solve and the solution could be slightly different. In this paper, we neglected this dependency, but still used the relation of mean and variance to estimate the variance of each pixel in the sinogram in advance: first, the mean of each pixel was evaluated using local windows, and then the variance was estimated according to equation (3).

A MAP estimation incorporated neighborhood information (the prior) into the equations and the low-pass property of the prior distribution regularized the resulted image to be smooth in any region. The parameter of the prior, α, is particular important, which controls the balance of the influence of the Gibbs prior and that of the likelihood, hence affects the image quality.

C. New Priori for Sinogram

It was noticed that the smoothing achieved by MAP method was mainly determined by the penalty term incorporated with the neighborhood information, which requires that the intensity of any specific pixel to be close to the intensities of its neighbors. For an unknown regular image, (e.g. a photo picture), this piece-wise smooth property is usually what we can only expected. However, for a sinogram image, we actually knew more than that. As illustrated in Fig. 2, the intensity of one pixel in a sinogram is determined by the object being scanned, which can be estimated from the whole sinogram. In another word, all pixels (i.e. projection rays) in the sinogram, not only its neighbors, provide useful information.

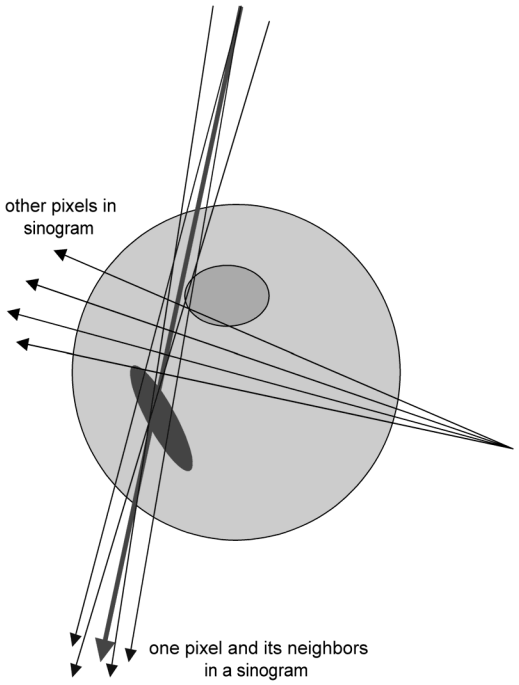

Fig. 2. Different property of a Sinogram from other piece-wise images. The intensity of one pixel in a sinogram is determined by the object being scanned, which can be estimated from the whole sinogram. Therefore, all rays, not only its neighbors, provide useful information.

Since any individual view of a sinogram contains information that contributes to other views, the data coming from relatively smooth area in the sinogram can be used to construct the *a priori* information when the noise reduction is performed in the relatively more noisy area (i.e., Fig. 1. regions A). For example, since the SNR of the projection at view angle 0^0 is much higher than that at view angle 90^0, (see Fig. 1. (b) and (c)), and they reflect some overlap information of the scanned object, it is better to apply this knowledge when we are smoothing the noise at view angle 90^0. Based on this observation, we incorporated a new *a priori* term into the

penalized WLS equation (10), as described by G in the following cost function:

$$\Phi(\mu) = \frac{1}{2}(X-\mu)^T \Sigma^{-1}(X-\mu) + \frac{1}{2}\mu^T H\mu + \beta G(\mu, \hat{X})$$

$$G(\mu, \hat{X}) = \frac{1}{2}\sum_{j\in A}(\mu_j - \hat{x}_j)^2 \qquad (12)$$

where $\hat{X}$ is an intermediate estimation for the data in noisy regions (labeled by A in Fig. 1.), which was calculated from the whole sinogram by re-projection.

The equations with the new prior term still have a closed-form analytical solution

$$\hat{\mu} = (\Sigma^{-1} + \alpha H + \beta I)^{-1}(\Sigma^{-1} X + \beta \hat{X}) \qquad (13)$$

and the data processing was very efficient.

III. Experimental Results

To validate our method, a shoulder phantom was scanned by the GE spiral CT scanner with fan-beam curved detector array. The distance from the center of rotation (COR) to the curved detector is 408.075 mm. The detector array is on an arc concentric to the X-ray source with a distance between the X-ray source and the COR equal to 541.00 mm. The detector cell spacing is 1.0239 mm. The protocol of 120kVp and 10mA was used for the scanning, and the number of channels per view was 888 with total 984 views evenly spanned on a circular orbit of 360^0. The detected photon number after system calibration and logarithm transform was our raw data, i.e. the sinogram showed in Fig. 1a.

The sinogram was first reconstructed by the conventional fan-beam filtered back-projection (FFBP) method with the Ramp filter, where streak artifacts were very clear, (see Fig. 3a). Secondly, we smoothed the sinogram with our proposed method, and reconstructed the processed sinogram with the same FFBP method. The result image was dramatically improved, where most of the artifacts were removed, see Fig. 3b and 3c (the difference image). The computational time for processing the sinogram, including variance calculation, intermediate sinogram estimation, and the penalized WLS with new prior smoothing, is is less than 1 minute at a PC Pentium 550Hz platform in this experiment.

IV. Discussions and Conclusions

The essential part of this method is the penalized term we added in, which preserves more accurate information when the extremely noisy region is being smoothed. This prior information comes from the unique characteristic of a sinogram image, and will not be applicable for other normal images. The processed sinogram after reconstruction by the conventional FFBP method showed dramatic improvements compared with original reconstructed image.

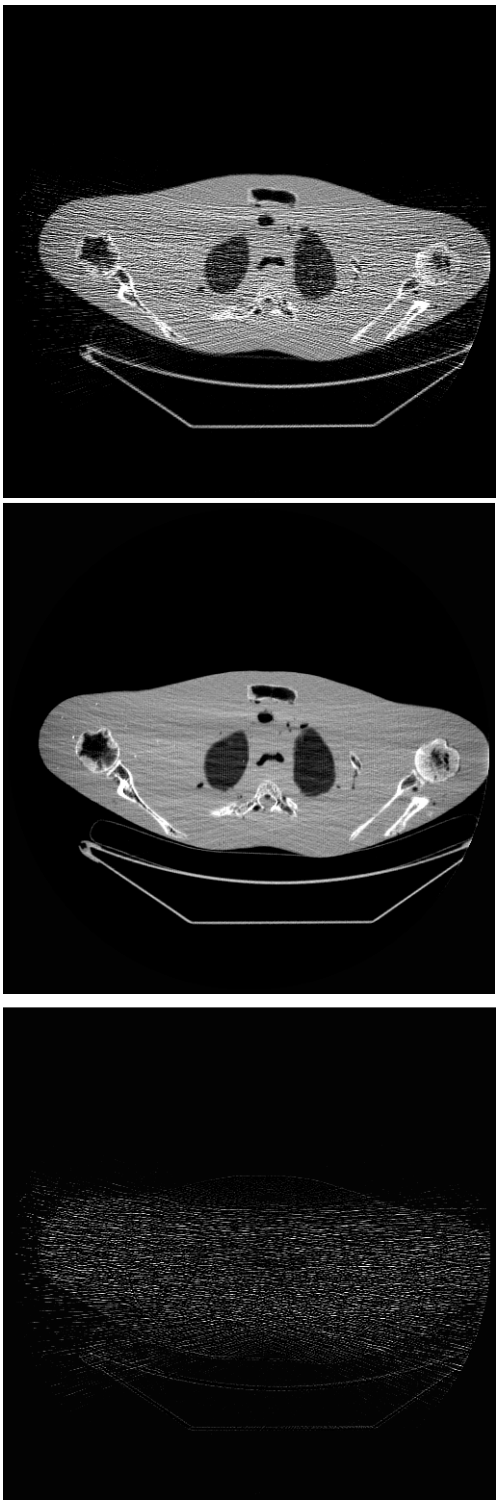

Fig. 3. Picture (a) is the reconstruction result from the original noisy data by FFBP method. Picture (b) is the FFBP reconstruction result with noise and streak artifacts reduction using the proposed method. Picture (c) is the difference image by subtracting (b) from (a).

Since the variance estimation is not optimized, (the dependence on the mean value was neglected), the MAP estimation become relatively simpler. In the future, the

variance and mean relation dependency may be incorporated in the statistic model, which may lead to different results.

V. REFERENCES

[1] J. Hsieh, "Adaptive streak artifact reduction in computed tomography resulting from excessive x-ray photon noise", Medical Physics, 25: 2139-2147, 1998.

[2] K. Demirkaya, "Reduction of noise and image artifacts in computed tomography by nonlinear filtration of the projection images", *SPIE Med. Imagin*g, **432**2, pp. 917-923, 2001.

[3] H. Lu, X. Li, I. T. Hsiao, and Z. Liang, "Analytical treatment of noise for low-dose CT projection data by penalized weighted least-square smoothing in the K-L domain", SPIE Medical Imaging, 4682: 146-152, 2002.

[4] T. Lei and W. Sewchand, "Statistical approach to x-ray CT imaging and its applications in image analysis - part I: Statistical analysis of x-ray CT imaging," IEEE Trans. Med. Imag., Vol. 11, March 1992.

[5] S. Geman and D. Geman, "Stochastic relaxation, Gibbs distributions and the Bayesian restoration of images," IEEE Trans. Pattern Analysis and Machine intelligence , vol. 6, no.7, pp. 721-741, July 1984.

[6] D. Lalush and B M W Tsui, "A generalized Gibbs prior for maximum aposteriori reconstruction in SPECT," Phys. Med. Biol. Vol. 38, pp. 729-741, 1993.

[7] J. A. Fessler, "Penalized weighted least-squares image reconstruction for positron emission tomography", IEEE Transaction on Medical Imaging, 13: 290-300, 1994.